

Post-Assembly Covalent Di- and Tetracapping of a Dinuclear $[\text{Fe}_2\text{L}_3]^{4+}$ Triple Helicate and Two $[\text{Fe}_4\text{L}_6]^{8+}$ Tetrahedra Using Sequential Reductive Aminations

Christopher R. K. Glasson,^{*,†} George V. Meehan,[†] Murray Davies,[†] Cherie A. Motti,[§] Jack K. Clegg,[‡] and Leonard F. Lindoy^{*,†,‡,‡}

[†]College of Science, Technology & Engineering, James Cook University, Townsville, Queensland 4811, Australia

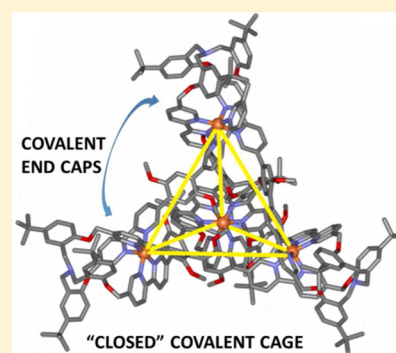
[§]The Australian Institute of Marine Science, Townsville, Queensland 4810, Australia

[‡]School of Chemistry and Molecular Biosciences, The University of Queensland, Brisbane St. Lucia, Queensland 4072 Australia

[#]School of Chemistry, The University of Sydney, Building F11 Eastern Avenue, Sydney, New South Wales 2006, Australia

S Supporting Information

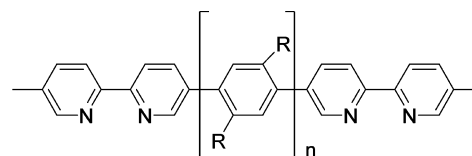
ABSTRACT: The use of a highly efficient reductive amination procedure for the postsynthetic end-capping of metal-templated helicate and tetrahedral supramolecular structures bearing terminal aldehyde groups is reported. Metal template formation of a $[\text{Fe}_2\text{L}_3]^{4+}$ dinuclear helicate and two $[\text{Fe}_4\text{L}_6]^{8+}$ tetrahedra (where L is a linear ligand incorporating two bipyridine domains separated by one or two 1,4-(2,5-dimethoxyaryl) linkers and terminated by salicylaldehyde functions) is described. Postassembly reaction of each of these “open” di- and tetranuclear species with excess ammonium acetate (as a source of ammonia) and sodium cyanoborohydride results in a remarkable reaction sequence whereby the three aldehyde groups terminating each end of the helicate, or each of the four vertices of the respective tetrahedra, react with ammonia then undergo successive reductive amination to yield corresponding fully tertiary-amine capped cryptate and tetrahedral covalent cages.



INTRODUCTION

Metallo-supramolecular assembly processes have now been employed to generate a truly impressive range of molecular architectures, often in a one-pot reaction and in high yield; the latter reflecting “error correction” associated with the relatively labile nature of the interactions typically employed in such assemblies.¹ In part, the success of such syntheses lies in component design that promotes the interaction of metal coordination and ligand sites to produce the desired metalloassembly. In many instances a further synthetic step (or steps) involving covalent modification of such preassembled structures has also been possible, allowing the facile preparation of many elaborate structures that would be difficult or impossible to obtain by conventional organic procedures. For example, such products include a wide variety of catenanes and rotaxanes,² cages,³ as well as an array of knots and related intertwined structures.⁴ Potential applications of the above structural categories are diverse and include such frontier research areas as molecular recognition and separation processes, catalysis, photonics, magnetic phenomena, molecular machines, and drug delivery technologies.⁵ Here we report the assembly of an extended $[\text{Fe}_2\text{L}_3]^{4+}$ triple helicate incorporating terminal aldehyde groups on each end of the ligand strands and its postassembly conversion to a dinuclear helical cryptate using an in situ (multiple) reductive amination procedure.⁶ On the basis of this result, the procedure was then adopted for the

preparation of a new category of tetracapped $[\text{Fe}_4\text{L}']^{8+}$ tetrahedral cages.



L^1 ; $n = 0$

L^2 ; $n = 1$, $\text{R} = \text{OCH}_3$

L^3 ; $n = 2$, $\text{R} = \text{OCH}_3$

Recently our group reported the synthesis of a series of discrete $[\text{M}_2\text{L}_3]^{4+}$ helicates and $[\text{M}_4\text{L}_6]^{8+}$ tetrahedra^{7–9} incorporating linear quaterpyridine derivatives of type L^1 – L^3 that in the case of particular tetrahedra exhibit interesting anion recognition behavior.^{10,11} The near-rigid 5,5''-dimethyl-2,2':5',5'':2'',2'''-quaterpyridine L^1 yields solely $[\text{Fe}_4(\text{L}^1)_6]^{8+}$ tetrahedra when reacted with a range of iron(II) salts. However, the extended systems L^2 and L^3 incorporating, respectively, dimethoxy-substituted 1,4-phenylene and tetramethoxy-substituted 4,4'-biphenylene bridges between the 2,2'-bipyridyl domains react with iron(II) or nickel(II) in a 3:2 ratio to

Received: May 4, 2015

Published: June 30, 2015

form $[M_2L_3]^{4+}$ and/or $[M_4L_6]^{8+}$ species, with the particular species being dependent on the experimental conditions employed (Figure 1).⁷ Such behavior, at least in part, was

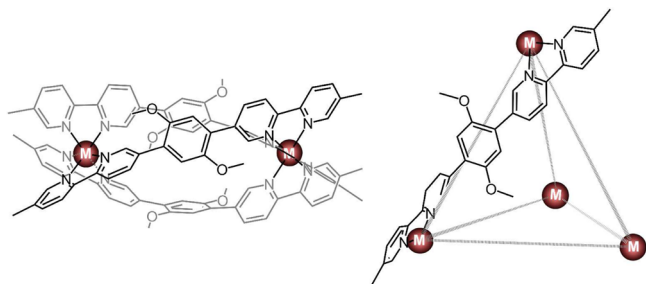


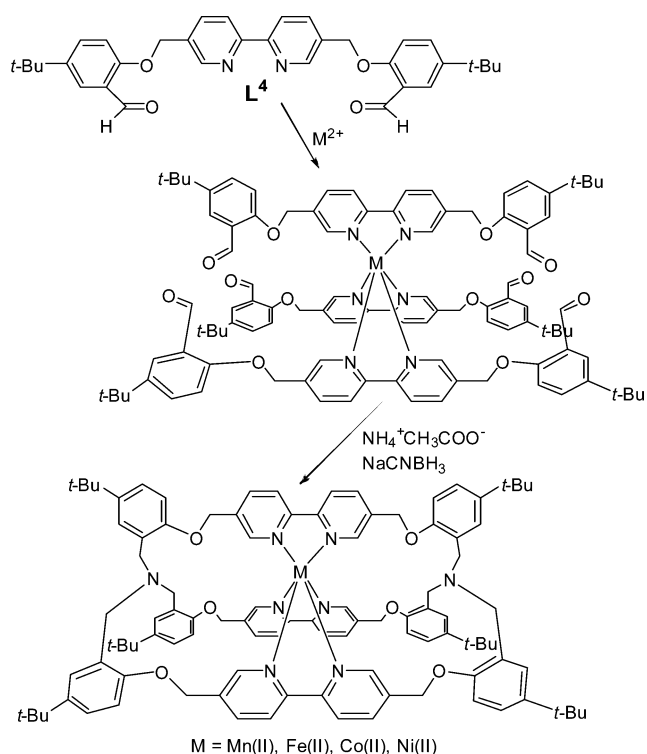
Figure 1. $[M_2(L^2)_3]^{4+}$ triple helicate (left) and $[M_4(L^2)_6]^{8+}$ tetrahedron (right) incorporating the semirigid linear quaterpyridyl L^2 .

attributed to the greater inherent flexibility of these latter extended quaterpyridines (relative to L^1). Thus, the use of dilute reaction conditions and/or a moderately short reaction time leads to enhanced yields of the $[M_2L_3]^{4+}$ species, consistent with these species being kinetic products, while longer reaction times and higher concentrations favored formation of $[M_4L_6]^{8+}$ species.

RESULTS AND DISCUSSION

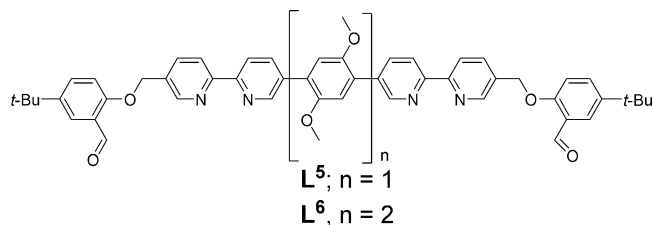
We have previously reported an efficient one-pot metal template procedure for synthesizing mononuclear tris-bipyridyl derivative cryptates of the type shown in Scheme 1.^{6,12} This procedure involved the reductive amination of tris-ligand $Mn(II)$, $Fe(II)$, $Co(II)$, and $Ni(II)$ complexes of the bipyridine derivative L^4 (Scheme 1) bearing terminal aldehyde groups. Each of these helical species was reacted with NH_4OAc (as an

Scheme 1. Synthesis of Divalent Metal Cryptates from L^4



ammonia source) and $NaCNBH_3$ to yield the corresponding doubly capped mononuclear cryptate. The outcome of this study, coupled with those involving L^1-L^3 discussed above,⁷ suggested the feasibility of generating larger closed species such as an extended dinuclear triple helical cryptate of type $[Fe_2(cryptand)]^{4+}$ or a closed tetranuclear tetrahedron cage of type $[Fe_4(cage)]^{8+}$. It was anticipated that successive reductive aminations involving three terminal aldehyde groups positioned at each end of the corresponding preassembled dinuclear helical precursor of type $[Fe_2(L^5)_3]^{4+}$, or at each of the four vertices of the similarly preassembled “open” tetrahedron of type $[Fe_4(L^5)_6]^{8+}$, might generate the corresponding closed dinuclear cryptate and tetranuclear cages, respectively.

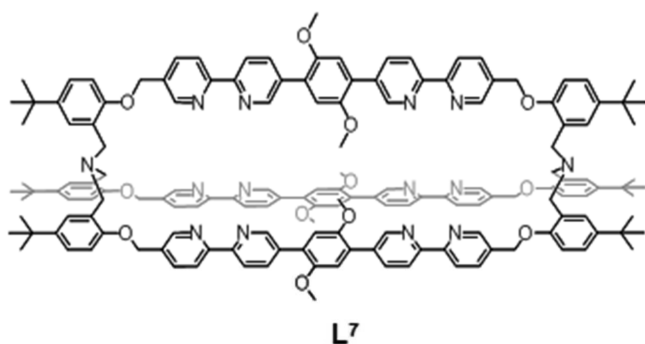
Accordingly, L^5 was prepared using a similar procedure to that reported for L^1 and L^2 ,⁷ with the exception that 2-((5'-bromo-[2,2'-bipyridin]-5-yl)methoxy)-5-(*tert*-butyl)-benzaldehyde was employed for the bis-Suzuki-coupling reaction with 2,2'-(2,5-dimethoxy-1,4-phenylene)bis(4,4,5,5-tetramethyl-1,3,2-dioxaborolane). The synthesis of the helical $[Fe_2(L^5)_3]^{4+}$ precursor was based on the conditions elucidated in our prior studies for differentiating between the formation of helical $[M_2L_3]^{4+}$ and tetrahedral $[M_4L_6]^{8+}$ species.⁷



$[Fe_2(L^5)_3]^{4+}$ was generated under dilute conditions and a reduced reaction time. The 1H NMR spectra of L^5 and $[Fe_2(L^5)_3](PF_6)_4$ are given in Supporting Information, Figure S1a,b, respectively. The latter spectrum is in accord with the ligand retaining its twofold symmetry within the complex. An AB system centered at 5.24 ppm is present indicating nonequivalent salicyloxymethylene protons due to restricted rotation (on the NMR time scale) around its associated carbon-carbon and carbon-oxygen σ -bonds. The high-resolution electrospray ionization mass spectrometry (HR-ESI-MS) of this product shows +2 and +3 ions corresponding to successive losses of PF_6^- from $[Fe_2(L^5)_3](PF_6)_4$.

Reductive amination of $[Fe_2(L^5)_3](PF_6)_4$ was performed by the reaction with NH_4OAc and $NaCNBH_3$ in acetonitrile at 0 °C. Following chromatography, the red $[Fe_2(L^7)]^{4+}$ cation was isolated as its PF_6^- salt in 60% yield. The 1H NMR spectrum of this product confirmed its symmetrical nature and showed the absence of an aldehyde proton peak at ~10 ppm [Supporting Information, Figure S1c]. The spectrum is in accord with the targeted structure; it contains an AB system centered at 3.20 ppm, corresponding to the methylene protons alpha to the nitrogen bridgehead atoms. The presence of a second AB system centered at 5.16 ppm is in keeping with the presence of restricted rotation around the $Ar-CH_2-O$ bonds of the salicyloxy moiety. The HR-ESI-MS revealed the presence of +2, +3, and +4 ions corresponding to the successive losses of PF_6^- counterions from $[Fe_2(L^7)](PF_6)_4$; the theoretical and observed isotopic distributions expected for $[Fe_2(L^7)]^{4+}$ are in excellent agreement (Supporting Information, Figure S2).

Hexagonal orange crystals of $[Fe_2(L^7)] \cdot 4PF_6 \cdot 30DMSO$ suitable for diffraction studies were obtained from a dimethyl sulfoxide (DMSO) solution after standing for several months.



The complex crystallizes (Figure 2) around a threefold axis with one-third of the molecule in the asymmetric unit. Each

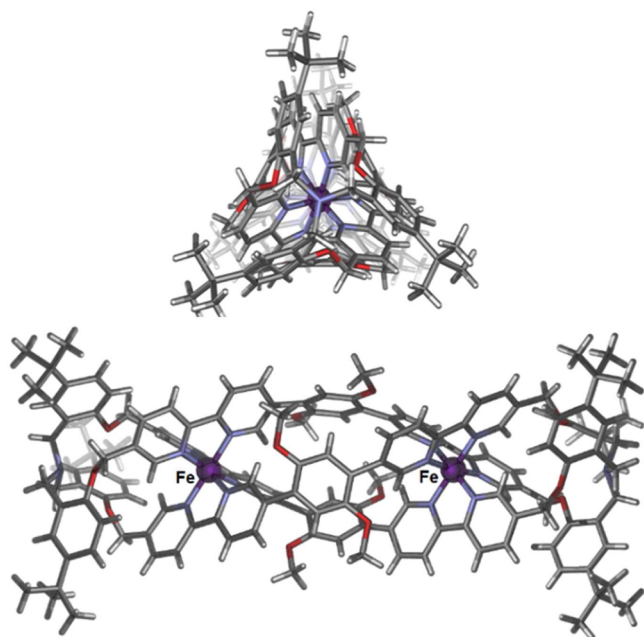


Figure 2. X-ray crystal structure of $[\text{Fe}_2(\text{L}^7)] \cdot 4\text{PF}_6 \cdot 30\text{DMSO}$. (upper) End view along the axis of the helix. (lower) Side view. Regions of disorder, anions, and solvents omitted for clarity.

octahedral iron(II) center has a tris-bipyridine coordination shell, with the two low-spin metal centers (Fe–N distances 1.95–1.99 Å) being separated by 11.5 Å. The metal centers within each complex are homochiral resulting in each discrete molecule having either $\Lambda\Lambda$ (*P*) or $\Delta\Delta$ (*M*) stereochemistry (overall, the sample is enantiomeric). The pitch of the helix extends the entire length of the molecule (25.7 Å) from bridgehead nitrogen–bridgehead nitrogen, both of which adopt an endo configuration. To adopt this arrangement the aromatic portion of each of the ligand strands is bent significantly ($\sim 36^\circ$) from planarity. This bend also results in a small encapsulated volume (29 Å³) inside the cryptate.

Motivated by the success of the above helical cage synthesis, the use of the $[\text{Fe}_4(\text{L}^5)]^{8+}$ assembly as a tetranuclear metallo-template precursor for closed tetrahedral cage formation was investigated. Reaction of iron(II) with L^5 in a 2:3 ratio under similar conditions to those reported previously⁷ for $[\text{Fe}_4(\text{L}^2)]^{8+}$ yielded $[\text{Fe}_4(\text{L}^5)](\text{PF}_6)_8$; the ¹H NMR spectrum was in accord with the target structure [see Supporting Information, Figure S3a,b]. Indicatively, an AB system centered at 5.17 ppm is present reflecting restricted rotation around Ar–

CH₂–O bonds of the salicyloxy moiety. The HR-ESI-MS of this product gave +5, +6, and +7 ions indicating losses of five, six, and seven PF₆[−] counterions from $[\text{Fe}_4(\text{L}^5)](\text{PF}_6)_8$.

Reductive amination of $[\text{Fe}_4(\text{L}^5)](\text{PF}_6)_8$ with NH₄OAc and NaCNBH₃ at 0 °C as described above for generating $[\text{Fe}_2(\text{L}^7)](\text{PF}_6)_4$ gave $[\text{Fe}_4(\text{L}^8)](\text{PF}_6)_8$ in 62% yield (Figure 3). The ¹H NMR spectrum indicated that the ligand had

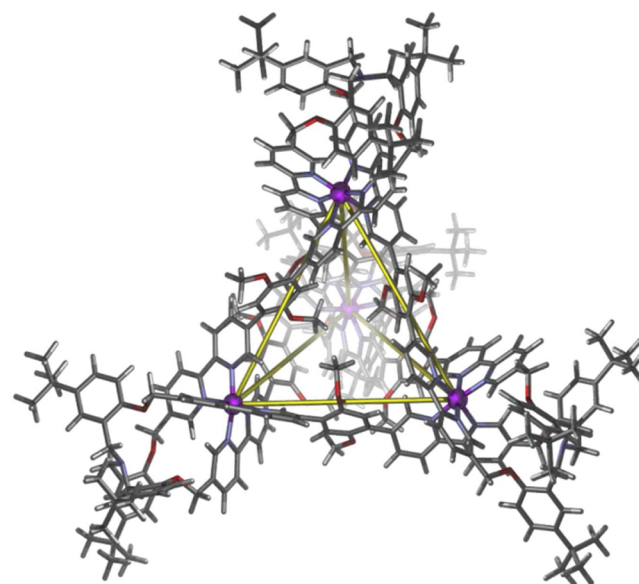


Figure 3. Structure of $[\text{Fe}_4(\text{L}^8)]^{8+}$ generated by molecular mechanics.

retained its twofold symmetry within the complex and that the aldehyde proton signal at ~ 10 ppm was no longer present. Instead, an AB system was now evident centered at 3.12 ppm arising from protons positioned alpha to the nitrogen bridgehead atoms [Supporting Information, Figure S3c]. HR-ESI-MS revealed +4, +5, and +6 ions corresponding to loss of four, five, and six PF₆[−] counterions from the formula $[\text{Fe}_4(\text{L}^8)](\text{PF}_6)_8$, respectively.

The excellent agreement between the theoretical and observed isotopic distributions for $\{[\text{Fe}_4(\text{L}^8)](\text{PF}_6)_3\}^{5+}$ is shown in Supporting Information, Figure S4. In forming the capped cage structure a total of 12 successive imine/iminium intermediates are sequentially formed and reduced—a total of 24 postassembly condensation/reduction steps takes place in forming this unprecedented closed tetrahedral cage species. An energy-minimized molecular model of $[\text{Fe}_4(\text{L}^8)]^{8+}$ is shown in Figure 3. The model is consistent with the spectroscopic results and closely agrees with the previously reported crystal structure of the $[\text{Fe}_4(\text{L}^2)]^{8+}$ parent.⁷ The model displays idealized *T*-symmetry with homochiral octahedral metal centers, which are separated by 12.99 Å. The organic components are similarly twisted into a chiral conformer such that each edge and capping tertiary amine adopts an identical atropisomer. The methoxy groups are orientated such that a number point inside the central cage cavity, restricting the potential void volume, while others lie on the faces of the tetrahedron and some point outward. We estimate that the guest accessible volume within the cage (based on the previous results obtained for $[\text{Fe}_4(\text{L}^5)]^{8+}$) is at least 227 Å³.⁷

In a parallel synthesis to the above, the precursor complex $[\text{Fe}_4(\text{L}^3)](\text{PF}_6)_8$ was prepared using a similar procedure to that employed for $[\text{Fe}_4(\text{L}^5)](\text{PF}_6)_8$. The ¹H NMR spectrum of

this product again indicated that the bound ligand retains its twofold symmetry, with an AB system centered at 5.21 ppm, once again indicating nonequivalence of the salicyloxy-methylene protons [Supporting Information, Figure S5a,b]. Reductive amination (as described above) of $[\text{Fe}_4(\text{L}^6)](\text{PF}_6)_8$ resulted in the generation of the corresponding tetracapped cage $[\text{Fe}_4(\text{L}^9)](\text{PF}_6)_8$ in 62% yield (Figure 4). The ^1H NMR

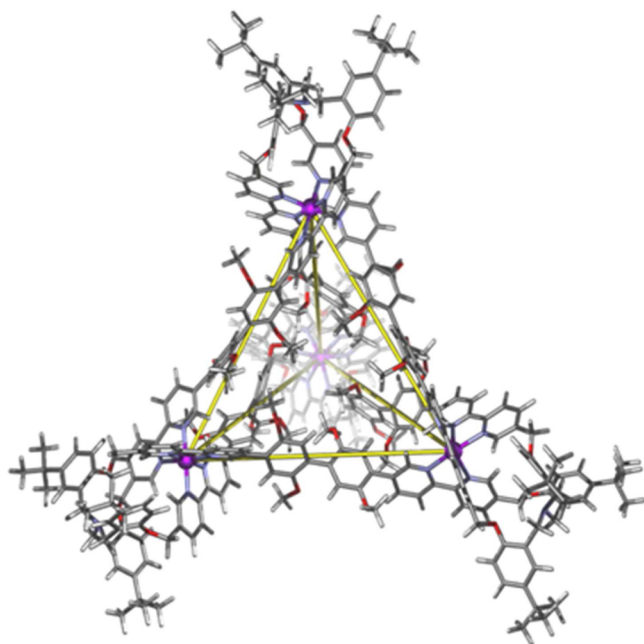


Figure 4. Structure of the $[\text{Fe}_4(\text{L}^9)]^{8+}$ tetrahedral cage based on a molecular mechanics minimized model of the cation.

spectrum of this product was in accord with the required fully capped tetrahedral cage structure and revealed that the aldehyde proton signal at ~ 10 ppm was no longer present; instead, an AB system centered at 3.15 ppm was evident, consistent with the nonequivalence of the two protons alpha to the nitrogen bridgehead atoms [Supporting Information, Figure S5c]. HR-ESI-MS of this product gave +4, +5, and +6 ions corresponding to the losses of PF_6^- counterions from $[\text{Fe}_4(\text{L}^9)](\text{PF}_6)_8$. Excellent agreement between the observed and theoretical isotopic distributions for $\{[\text{Fe}_4(\text{L}^9)](\text{PF}_6)_3\}^{5+}$ was again obtained (Supporting Information, Figure S6). Again the molecular model of $[\text{Fe}_4(\text{L}^9)]^{8+}$ is in excellent agreement with both the crystal structure of $[\text{Fe}_4(\text{L}^6)]^{8+}$ and the spectroscopic data. The structure shows idealized T -symmetry and a metal–metal separation of 17.48 Å. The metal ions show homochirality within each assembly, and the L^9 ligand is also twisted into a chiral conformation. The volume encapsulated by the cage is estimated to exceed 417 Å³ based on previous studies.⁷

CONCLUSION

In conclusion, we have exemplified the use of an efficient reductive amination procedure for the postsynthetic end-capping of metal templated helicate and tetrahedral supramolecular structures bearing terminal aldehyde groups. The successful formation of such capped tetrahedrons gives rise to the first members of a new category of covalently closed cages—in this work isolated as their tetra-iron(II) derivatives. Clearly, the successful outcome of the present study points the way for

further application of the reductive amination process for constructing related closed topologies such as molecular boxes and the like.

EXPERIMENTAL SECTION

Materials and Methods. All reagents were of analytical grade unless otherwise indicated. Chromatography-grade solvents were distilled through a fractionation column packed with glass helices. ^1H and ^{13}C NMR spectra were recorded on a Bruker AM-300 or a Varian Mercury 300 MHz spectrometer (300.133 MHz) at 298 K. ^1H and ^{13}C NMR resonance are quoted in parts per million, and the coupling constants (J) are given in hertz. ^1H NMR spectra were referenced with respect to the residual proton resonances for CDCl_3 (7.24 ppm) and CD_3CN (1.94 ppm). ^{13}C NMR spectra were referenced to solvent peaks for CDCl_3 (77.0 ppm) and CD_3CN (1.39 ppm). Positive-ion high-resolution electrospray ionization (HR-ESI): Fourier transform ion cyclotron resonance mass spectrometry (FTICR-MS) measurements were obtained on a Bruker BioAPEX 47e mass spectrometer equipped with an Analytica of Branford electrospray ionization source. The optimized molecular mechanics models of the tetrahedral cages were generated using SPARTAN '14 employing the SYBYL force field;¹³ starting coordinates were based on those for a combination of the previously determined X-ray structures of the parent “open” tetrahedra⁷ and terminal capping groups taken from the helical cryptate structure described in the present communication.

Organic Synthesis. Radical halogenation of 5'-bromo-5-methyl-2,2'-bipyridine using *N*-bromosuccinimide (NBS) afforded 5'-bromo-5-bromomethyl-2,2'-bipyridine in 64% yield. 2-(5'-Bromo-[2,2']-bipyridinyl-5-ylmethoxy)-5-*tert*-butyl-benzaldehyde (Supporting Information, Scheme S1) was prepared in 90% yield by *O*-alkylation of 5-*tert*-butyl-2-hydroxybenzaldehyde with 5'-bromo-5-bromomethyl-2,2'-bipyridine under basic conditions in dimethylformamide (DMF).

The syntheses of the dimethoxyphenylene and tetramethoxybiphenylene bridged dialdehyde derivatives, L^5 and L^6 (see Supporting Information, Scheme S1), were achieved by bis-Suzuki coupling reactions of 2-(5'-bromo-[2,2']bipyridinyl-5-ylmethoxy)-5-*tert*-butyl-benzaldehyde to bis-boronic esters, 1,4'-bis(4,4,5,5-tetramethyl[1,3,2]-dioxaborolan)-2,5-dimethoxybenzene and 4,4'-bis(4,4,5,5-tetramethyl[1,3,2]-dioxaborolan)-1,1'-(2,2',5,5'-tetramethoxy)biphenyl L^5 and L^6 were characterized via ^1H and ^{13}C NMR spectra, and positive-mode HR-ESI-MS was used to confirm their composition.

Ligand Syntheses. 5'-Bromo-5-bromomethyl-2,2'-bipyridine: A solution of 5'-bromo-5-methyl-2,2'-bipyridine (2.49 g, 10 mmol) and NBS (1.78 g, 10 mmol) in CCl_4 (40 cm³) was irradiated with a broad spectrum tungsten white light while under reflux for 30 min. The CCl_4 was removed, H_2O (40 cm³) was added, and the mixture was stirred for 0.5 h. Following filtration of the mixture the solid was washed with a minimum amount of water, chilled methanol, and then ether. The resulting product was chromatographed on silica gel with petrol (40%) and dichloromethane (DCM, 60%) as eluent to afford the product (2.1 g, 64%) as a white solid. ^1H NMR (300 MHz, chloroform-*d*₃) δ 8.72 (d, $J = 2.4$ Hz, 1H), 8.67 (d, $J = 2.4$ Hz, 1H), 8.37 (d, $J = 8.1$ Hz, 1H), 8.32 (d, $J = 8.7$ Hz, 1H), 7.94 (dd, $J = 8.7, 2.4$ Hz, 1H), 7.85 (dd, $J = 8.1, 2.4$ Hz, 1H), 4.53 (s, 2H); ^{13}C NMR (75 MHz, chloroform-*d*₃) δ 155.18, 154.04, 150.52, 149.46, 139.83, 138.09, 134.28, 122.83, 122.76, 121.25, 29.93; HR-ESI-MS (DCM/MeOH): m/z calcd for $\text{C}_{11}\text{H}_9\text{Br}_2\text{N}_2$ $[M+\text{H}]^+$ 326.9128, found 326.9137; calcd for $\text{C}_{11}\text{H}_8\text{Br}_2\text{N}_2\text{Na}$ $[M+\text{Na}]^+$ 348.8947, found 348.8959.

2-(5'-Bromo-[2,2']bipyridinyl-5-ylmethoxy)-5-*tert*-butyl-benzaldehyde. A DMF (15 cm³) solution of 5-*tert*-butyl-2-hydroxybenzaldehyde (214 mg, 1.2 mmol) and 5'-bromo-5-bromomethyl-2,2'-bipyridine (328 mg, 1 mmol) in the presence of K_2CO_3 (414 mg, 3 mmol) was stirred at room temperature over 10 h. H_2O (25 cm³) was then added to the reaction mixture, and the resulting precipitate was removed by filtration and washed with water followed by a minimum volume of chilled MeOH. The crude product was purified by chromatography on silica gel with DCM (98.75%), MeOH (1%), and saturated NH_3 (0.25%) as eluent to afford the product (383 mg, 90%)

as a white solid. ^1H NMR (300 MHz, chloroform- d_3) δ 10.54 (s, 1H), 8.75 (d, J = 2.4 Hz, 1H), 8.75 (d, J = 2.7 Hz, 1H), 8.44 (d, J = 7.8 Hz, 1H), 8.36 (d, J = 8.4 Hz, 1H), 7.96 (dd, J = 8.4, 2.7 Hz, 1H), 7.94 (dd, J = 7.8, 2.4 Hz, 1H), 7.89 (d, J = 2.7 Hz, 1H), 7.59 (dd, J = 9.0, 2.7 Hz, 1H), 7.01 (d, J = 9.0 Hz, 1H), 5.25 (s, 2H), 1.32 (s, 9H); ^{13}C NMR (75 MHz, chloroform- d_3) δ 189.85, 158.69, 155.20, 153.98, 150.54, 148.22, 144.69, 139.85, 136.66, 133.36, 132.55, 125.59, 124.80, 122.74, 121.69, 121.31, 112.79, 68.16, 34.54, 31.49; HR-ESI-MS (DCM/MeOH): m/z calcd for $\text{C}_{22}\text{H}_{22}\text{BrN}_2\text{O}_2$ $[\text{M} + \text{H}]^+$ 425.0859, found 425.0849; calcd for $\text{C}_{22}\text{H}_{21}\text{BrN}_2\text{O}_2\text{Na}$ $[\text{M} + \text{Na}]^+$ 447.0679, found 447.0663.

1,4-Bis[5'-(5''-(2-formyl-4-tert-butylphenoxy)methyl)-2',2''-bipyridinyl]-2,5-dimethoxybenzene (L^5). A solution of 2-(5'-bromo-[2,2']bipyridinyl-5-ylmethoxy)-5-tert-butyl-benzaldehyde (950 mg, 2.2 mmol), 1,4'-bis(4,4,5,5-tetramethyl[1,3,2]dioxaborolan)-2,5-dimethoxybenzene (390 mg, 1.0 mmol), and Na_2CO_3 (910 mg, 6.6 mmol, dissolved in 7 cm^3 H_2O) in DMF (14 cm^3) was degassed with N_2 . $\text{Pd}(\text{PPh}_3)_4$ (70 mg, 0.06 mmol) was added to this solution, and the reaction mixture was heated with microwave energy in a sealed pressurized microwave vessel with temperature and pressure sensors and a magnetic stirrer bar (Step 1—the temperature was ramped to 120 $^\circ\text{C}$ over 2 min using 100% of 400 W; Step 2—the solution was held at 120 $^\circ\text{C}$ for 8–20 min using 30% of 400 W). H_2O (20 cm^3) was added, and the resulting precipitate was isolated by filtration and washed with H_2O . The crude product was recrystallized from DMF/ H_2O to afford the product (766 mg, 93%) as a pale yellow crystalline solid. ^1H NMR (300 MHz, chloroform- d_3) δ 10.55 (s, 2H), 8.92 (d, J = 2.4 Hz, 2H), 8.79 (d, J = 2.1 Hz, 2H), 8.54 (d, J = 8.1 Hz, 2H), 8.52 (d, J = 8.4 Hz, 2H), 8.10 (dd, J = 8.4, 2.4 Hz, 2H), 7.96 (dd, J = 8.1, 2.1 Hz, 2H), 7.87 (d, J = 2.7 Hz, 2H), 7.64 (dd, J = 8.7, 2.7 Hz, 2H), 7.12 (s, 2H), 7.09 (d, J = 8.7 Hz, 2H), 5.29 (s, 4H), 3.87 (s, 6H), 1.33 (s, 18H). ^{13}C NMR (75 MHz, chloroform- d_3) δ 189.62, 158.90, 156.17, 154.35, 151.33, 149.83, 148.58, 144.49, 137.78, 136.38, 134.26, 133.32, 132.23, 127.65, 125.13, 124.84, 120.88, 120.39, 114.41, 112.97, 68.39, 56.58, 34.39, 31.21; HR-ESI-MS (DCM/MeOH): m/z calcd for $\text{C}_{52}\text{H}_{51}\text{N}_4\text{O}_6$ $[\text{M} + \text{H}]^+$ 827.3725, found 827.3725; calcd for $\text{C}_{52}\text{H}_{50}\text{N}_4\text{O}_6\text{Na}$ $[\text{M} + \text{Na}]^+$ 849.3647, found 849.3647.

4,4'-Bis[5''-(5'''-(2-formyl-4-tert-butylphenoxy)methyl)-2'',2'''-bipyridinyl]-1,1'-(2,2',5,5'-tetramethoxy)biphenyl (L^6). The procedure was similar to that used for the synthesis of 1,4-bis[5'-(5''-(2-formyl-4-tert-butylphenoxy)methyl)-2',2''-bipyridinyl]-2,5-dimethoxybenzene employing 2-(5'-bromo-[2,2']bipyridinyl-5-ylmethoxy)-5-tert-butyl-benzaldehyde (260 mg, 0.68 mmol), 4,4'-bis(4,4,5,5-tetramethyl[1,3,2]dioxaborolan)-1,1'-(2,2',5,5'-tetramethoxy)biphenyl (163 mg, 0.31 mmol), K_2CO_3 (250 mg, 1.8 mmol, in 5 cm^3 H_2O), and $\text{Pd}(\text{PPh}_3)_4$ (20 mg, 0.018 mmol) in DMF (10 cm^3). The crude product was recrystallized from DMF/ H_2O to afford the product (260 mg, 87%) as a pale yellow crystalline solid. ^1H NMR (300 MHz, chloroform- d_3) δ 10.57 (s, 2H), 8.95 (d, J = 2.2 Hz, 2H), 8.78 (d, J = 2.2 Hz, 2H), 8.51 (d, J = 8.2 Hz, 2H), 8.47 (d, J = 8.0 Hz, 2H), 8.09 (dd, J = 8.2, 2.2 Hz, 2H), 7.94 (dd, J = 8.0, 2.2 Hz, 2H), 7.91 (d, J = 2.6 Hz, 2H), 7.60 (dd, J = 8.7, 2.6 Hz, 2H), 7.07 (s, 4H), 7.05 (s, 4H), 7.03 (d, J = 8.7 Hz, 2H), 5.28 (s, 4H), 3.86 (s, 6H), 3.84 (s, 6H), 1.33 (s, 18H). ^{13}C NMR (75 MHz, chloroform- d_3) δ 189.62, 158.91, 156.24, 154.21, 151.64, 150.73, 149.88, 148.58, 144.49, 137.81, 136.37, 134.56, 133.31, 132.18, 128.35, 126.85, 125.12, 124.85, 120.86, 120.37, 115.57, 114.00, 112.98, 68.41, 56.67, 56.54, 34.39, 31.22; HR-ESI-MS (DCM/MeOH): m/z calcd for $\text{C}_{60}\text{H}_{59}\text{N}_4\text{O}_8$ $[\text{M} + \text{H}]^+$ 963.4333, found 963.4277; calcd for $\text{C}_{60}\text{H}_{58}\text{N}_4\text{O}_8\text{Na}$ $[\text{M} + \text{Na}]^+$ 985.4152, found 985.4089.

Complex Synthesis. $[\text{Fe}_2(\text{L}^5)](\text{PF}_6)_4$. A stirred solution of $\text{Fe}(\text{BF}_4)_2 \cdot 6\text{H}_2\text{O}$ (13.6 mg, 0.040 mmol) and L^5 (175 mg, 0.212 mmol) in CH_3CN (250 cm^3) was refluxed for 1.5 h. The solvent was then removed under vacuum, and the crude material was purified by chromatography on silica gel with CH_3CN , H_2O , and saturated KNO_3 (7:1:0.5) as eluent. The major product was isolated by precipitation with excess aqueous KPF_6 in H_2O (20 cm^3) followed by filtration to afford the M_2L_3 precursor complex (90 mg, 40%) as a red solid. ^1H NMR (300 MHz, acetonitrile- d_3) δ 10.01 (s, 6H), 8.64 (d, J = 8.5 Hz, 6H), 8.55 (d, J = 8.3 Hz, 6H), 8.44 (d, J = 7.9 Hz, 6H), 8.22 (dd, J =

8.3, 1.6 Hz, 6H), 7.75 (d, J = 2.6 Hz, 6H), 7.67 (s, 6H), 7.63 (dd, J = 8.8, 2.7 Hz, 6H), 7.30 (s, 6H), 6.98 (d, J = 8.8 Hz, 6H), 6.80 (s, 6H), 5.27 (d, J = 14.0 Hz, 6H), 5.21 (d, J = 14.0 Hz, 6H), 3.52 (s, 18H), 1.29 (s, 54H); ^{13}C NMR (75 MHz, acetonitrile- d_3) δ 189.91, 159.09, 158.93, 154.67, 153.31, 151.31, 145.59, 138.67, 138.65, 138.35, 137.78, 137.63, 134.55, 126.16, 125.87, 125.49, 125.12, 124.75, 117.06, 114.04, 68.00, 58.36, 34.96, 31.46; HR-ESI-MS (DCM/MeOH): m/z calcd for $[\text{Fe}_2(\text{L}^5)_3](\text{PF}_6)_3$ $^{2+}$, $[\text{M} - 2\text{PF}_6]^{2+}$ 1440.9601, found 1440.9688; calcd for $\{[\text{Fe}_2(\text{L}^5)](\text{PF}_6)\}^{3+}$, $[\text{M} - 3\text{PF}_6]^{3+}$ 912.3185, found 912.3199.

$[\text{Fe}_4(\text{L}^5)]_6(\text{PF}_6)_8$. A stirred solution of L^5 (91 mg, 0.110 mmol) and $\text{FeCl}_2 \cdot 5\text{H}_2\text{O}$ (16 mg, 0.073 mmol) in acetonitrile (10 cm^3) was heated using microwave energy in a sealed pressurized microwave vessel with temperature and pressure sensors attached (Step 1—ramped to 120 $^\circ\text{C}$ over 2 min using 100% of 400 W; Step 2—held at 120 $^\circ\text{C}$ for 40 min using 25% of 400 W). The crude product was purified by chromatography on silica gel with CH_3CN , H_2O , and saturated KNO_3 (7:1:0.5) as eluent. An aqueous solution of KPF_6 was added to the major fraction, which afforded the M_4L_6 precursor complex (110 mg, 95%) as a red solid. ^1H NMR (300 MHz, acetonitrile- d_3) δ 9.90 (s, 12H), 8.56 (d, J = 5.2 Hz, 12H), 8.53 (d, J = 5.1 Hz, 12H), 8.36–8.27 (m, 12H), 8.15 (dd, J = 8.4, 1.4 Hz, 12H), 8.11–8.09 (m, 12H), 7.73 (d, J = 2.6 Hz, 12H), 7.60 (dd, J = 8.8, 2.7 Hz, 12H), 7.53 (d, J = 1.8 Hz, 12H), 6.92 (d, J = 8.9 Hz, 12H), 6.88 (s, 12H), 5.21 (d, J = 14.0 Hz, 12H), 5.13 (d, J = 14.0 Hz, 12H), 3.35 (s, 36H), 1.27 (s, 108H). ^{13}C NMR (75 MHz, CD_3CN): δ = 189.70, 160.58, 159.29, 157.50, 155.16, 152.43, 152.29, 150.74, 139.95, 138.38, 137.95, 137.60, 137.30, 129.57, 125.69, 124.55, 124.48, 122.66, 116.75, 114.19, 67.63, 56.98, 34.73, 31.52; HR-ESI-MS (pos. mode, DCM/MeOH): m/z calcd for $\{[\text{Fe}_4(\text{L}^5)_6](\text{PF}_6)_3\}^{5+}$: $[\text{M} - 5\text{PF}_6]^{5+}$ 1123.9758, found 1123.9894; calcd for $\{[\text{Fe}_4(\text{L}^5)]_6(\text{PF}_6)_2\}^{6+}$: $[\text{M} - 6\text{PF}_6]^{6+}$ 912.4857, found 912.4910; calcd for $\{[\text{Fe}_4(\text{L}^5)]_6(\text{PF}_6)\}^{7+}$: $[\text{M} - 7\text{PF}_6]^{7+}$ 761.4213, found 761.4279.

$[\text{Fe}_4(\text{L}^6)]_6(\text{PF}_6)_8$. A stirred solution of L^6 (24 mg, 0.025 mmol) and $\text{Fe}(\text{BF}_4)_2 \cdot 6\text{H}_2\text{O}$ (5.6 mg, 0.0167 mmol) in acetonitrile (10 cm^3) was heated using microwave energy in a sealed pressurized microwave vessel with temperature and pressure sensors (Step 1—ramped to 120 $^\circ\text{C}$ over 2 min using 100% of 400 W; Step 2—held at 120 $^\circ\text{C}$ for 40 min using 25% of 400 W). The crude product was purified by chromatography on silica gel with CH_3CN , H_2O , and saturated KNO_3 (7:1:0.5) as eluent to afford $[\text{Fe}_4(\text{L}^6)]_6(\text{PF}_6)_8$ (27 mg, 91%) as a red solid. ^1H NMR (300 MHz, acetonitrile- d_3) δ 9.92 (s, 12H), 8.57 (m, 24H), 8.32 (d, J = 8.6 Hz, 12H), 8.19 (d, J = 8.6 Hz, 12H), 7.78 (s, 12H), 7.73 (d, J = 2.6 Hz, 12H), 7.67 (s, 12H), 7.62 (dd, J = 8.8, 2.6 Hz, 12H), 6.96 (d, J = 8.9 Hz, 12H), 6.87 (s, 12H), 6.86 (s, 12H), 5.25 (d, J = 14.1 Hz, 12H), 5.17 (d, J = 14.1 Hz, 12H), 3.58 (s, 36H), 3.43 (s, 36H), 1.28 (s, 108H); ^{13}C NMR (75 MHz, acetonitrile- d_3) δ 189.74, 159.41, 158.85, 157.71, 155.27, 152.83, 152.27, 150.73, 145.43, 138.40, 137.93, 134.56, 134.03, 129.55, 125.72, 124.95, 124.49, 124.40, 116.68, 114.38, 113.88, 67.79, 57.01, 56.96, 34.89, 31.39; HR-ESI-MS (DCM/MeOH): m/z calcd for $[\text{Fe}_4(\text{L}^6)]_6(\text{PF}_6)_4$ $[\text{M} - 4\text{PF}_6]^{4+}$ 1645.2897, found 1645.2743; calcd for $\{[\text{Fe}_4(\text{L}^6)]_6(\text{PF}_6)_3\}^{5+}$, $[\text{M} - 5\text{PF}_6]^{5+}$ 1287.2369, found 1287.2277; calcd for $\{[\text{Fe}_4(\text{L}^6)]_6(\text{PF}_6)_2\}^{6+}$, $[\text{M} - 6\text{PF}_6]^{6+}$ 1048.5383, found 1048.5332.

$[\text{Fe}_2(\text{L}^7)](\text{PF}_6)_4$. A solution of $[\text{Fe}_2(\text{L}^5)](\text{PF}_6)_4$ (60 mg, 0.019 mmol) and NH_4OAc (60 mg, 0.760 mmol) in acetonitrile (50 cm^3) stirred for 0.5 h at room temperature. The reaction mixture was then cooled to 0 $^\circ\text{C}$ in an ice bath (to inhibit reduction of the aldehydes to the corresponding benzylic alcohols) before the addition of NaCNBH_3 (24 mg, 0.380 mmol). After 1 h the reaction mixture was allowed to warm to room temperature and stirred overnight. Following this, the solvent volume was reduced under vacuum to ~ 5 cm^3 , and excess KPF_6 in H_2O (15 cm^3) was added. The resulting precipitate was isolated by filtration and washed with H_2O and a minimum volume of cold MeOH. The crude product was purified by chromatography on silica gel with CH_3CN , H_2O , and saturated KNO_3 (7:1:0.5) as eluent. An aqueous solution of KPF_6 was added to the major fraction, which afforded the dinuclear cryptate (35 mg, 60%) as a red solid. ^1H NMR (300 MHz, acetonitrile- d_3) δ 8.73 (d, J = 8.5 Hz, 6H), 8.66 (d, J = 8.3 Hz, 6H), 8.48 (d, J = 8.5 Hz, 6H), 8.19 (s, 6H), 8.06 (d, J = 8.3 Hz,

6H), 7.34 (dd, $J = 8.6, 2.5$ Hz, 6H), 7.31 (s, 6H), 7.05 (d, $J = 2.5$ Hz, 6H), 6.95 (d, $J = 8.6$ Hz, 6H), 6.82 (s, 6H), 5.00 and 5.31 (AB system, $d, J_{AB} = 13.5$ Hz, CH₂O, 6H each), 3.55 (s, 18H), 3.12 and 3.29 (AB system, $d, J_{AB} = 11.5$ Hz, CH₂N, 6H each), 1.27 (s, 54H). ¹³C NMR (75 MHz, acetonitrile-*d*₃) δ 159.32, 159.00, 156.51, 154.47, 153.81, 151.35, 145.69, 139.64, 138.29, 137.75, 137.60, 129.40, 128.40, 126.40, 126.11, 125.62, 124.72, 117.06, 113.39, 69.04, 58.43, 51.82, 34.77, 31.69; HR-ESI-MS (pos. mode, DCM/MeOH): m/z calcd for $\{[\text{Fe}_2(\text{L}^7)(\text{PF}_6)_2]^{2+}, [\text{M} - 2\text{PF}_6]^{2+}$ 1410.0019, found 1410.0003; calcd for $\{[\text{Fe}_2(\text{L}^7)(\text{PF}_6)_3]^{3+}, [\text{M} - 3\text{PF}_6]^{3+}$ 891.6797, found 891.6845; calcd for $[\text{Fe}_2(\text{L}^7)]^{4+}, [\text{M} - 4\text{PF}_6]^{4+}$ 632.5186, found 632.5206. A crystalline sample of the above product was obtained by recrystallization from DMF over several months, and the product was further characterized by an X-ray structure determination.

$[\text{Fe}_4(\text{L}^8)](\text{PF}_6)_8$. A solution of $[\text{Fe}_4(\text{L}^8)](\text{PF}_6)_8$ (40 mg, 0.0076 mmol) and NH₄OAc (78 mg, 1.0 mmol) in acetonitrile (50 cm³) was stirred at room temperature for 0.5 h. The reaction mixture was cooled to 0 °C in an ice bath prior to the addition of NaCNBH₃ (62 mg, 1.0 mmol). This reaction mixture was held at 0 °C for 2 h before warming to room temperature and was stirred overnight. The volume was then reduced under vacuum to ~10 cm³, and the product was precipitated by addition of an excess of KPF₆ in H₂O (20 cm³). The crude product was isolated by filtration and purified by chromatography on silica gel with CH₃CN, H₂O, and saturated KNO₃ (7:1:0.5) as eluent to afford $[\text{Fe}_4(\text{L}^8)](\text{PF}_6)_4$ (32 mg, 62%) as a red solid. ¹H NMR (300 MHz, acetonitrile-*d*₃) δ 8.70 (d, $J = 8.1$ Hz, 12H), 8.66 (d, $J = 8.1$ Hz, 12H), 8.45 (dd, $J = 8.6, 2.0$ Hz, 12H), 8.11 (d, $J = 2.0$ Hz, 12H), 8.04 (dd, $J = 8.4, 1.8$ Hz, 12H), 7.35 (dd, $J = 8.6, 2.6$ Hz, 12H), 7.10 (d, $J = 2.6$ Hz, 12H), 6.96 (d, $J = 1.8$ Hz, 12H), 6.93 (s, 12H), 4.99 and 5.26 (AB system, $d, J_{AB} = 13.5$ Hz, CH₂O, 12H each), 3.48 (s, 36H), 3.07 and 3.17 (AB system, $d, J_{AB} = 12.0$ Hz, CH₂N, 12H each), 1.29 (s, 108H); ¹³C NMR (75 MHz, CD₃CN): $\delta = 159.16, 158.48, 156.34, 155.40, 153.50, 152.03, 145.53, 139.47, 139.17, 138.22, 136.89, 129.33, 128.19, 126.35, 125.91, 124.61, 124.48, 114.97, 113.09, 68.72, 57.48, 34.73, 31.66$; HR-ESI-MS (DCM/MeOH): m/z calcd for $[\text{Fe}_4(\text{L}^8)](\text{PF}_6)_4$ $[\text{M} - 4\text{PF}_6]^{4+}$ 1410.2527, found 1410.2611; calcd for $\{[\text{Fe}_4(\text{L}^8)](\text{PF}_6)_3\}^{5+}, [\text{M} - 3\text{PF}_6]^{5+}$ 1099.2092, found 1099.2198; calcd for $\{[\text{Fe}_4(\text{L}^8)](\text{PF}_6)_2\}^{6+}, [\text{M} - 2\text{PF}_6]^{6+}$ 891.8469, found 891.8559.

$[\text{Fe}_4(\text{L}^9)](\text{PF}_6)_8$. A solution of $[\text{Fe}_4(\text{L}^9)](\text{PF}_6)_8$ (27 mg, 0.0038 mmol) and NH₄OAc (39 mg, 0.5 mmol) in acetonitrile (50 cm³) was stirred at room temperature for 0.5 h. The reaction mixture was cooled to 0 °C in an ice bath prior to the addition of NaCNBH₃ (31 mg, 0.5 mmol). This reaction mixture was held at 0 °C for 2 h before warming to room temperature and was stirred overnight. The volume was then reduced under vacuum to ~10 cm³, and the product was precipitated by addition of an excess of NH₄PF₆ in H₂O (20 cm³). The crude product was isolated by filtration and purified by chromatography on silica gel with CH₃CN, H₂O, and saturated KNO₃ (7:1:0.5) as eluent to afford $[\text{Fe}_4(\text{L}^9)](\text{PF}_6)_8$ (16 mg, 62%) as a red solid. ¹H NMR (300 MHz, acetonitrile-*d*₃) δ 8.66 (d, $J = 8.5$ Hz, 12H), 8.63 (d, $J = 8.4$ Hz, 12H), 8.37 (dd, $J = 8.5, 2.0$ Hz, 12H), 8.17 (d, $J = 1.7$ Hz, 12H), 8.02 (dd, $J = 8.4, 1.7$ Hz, 12H), 7.80 (d, $J = 2.0$ Hz, 12H), 7.32 (dd, $J = 8.6, 2.6$ Hz, 12H), 7.07 (d, $J = 2.6$ Hz, 12H), 6.91 (d, $J = 8.6$ Hz, 12H), 6.89 (s, 12H), 6.87 (s, 12H), 4.98 and 5.22 (AB system, $d, J_{AB} = 12.0$ Hz, CH₂O, 12H each), 3.63 (s, 36H), 3.47 (s, 36H), 3.07 and 3.22 (AB system, $d, J_{AB} = 11.6$ Hz, CH₂N, 12H each), 1.26 (s, 108H); ¹³C NMR (75 MHz, acetonitrile-*d*₃) δ 158.38, 157.17, 155.33, 154.16, 152.50, 151.38, 149.81, 144.52, 139.03, 138.21, 137.15, 136.96, 128.67, 128.43, 127.13, 125.40, 123.60, 123.56, 115.79, 113.53, 111.97, 111.43, 67.67, 56.12, 56.02, 50.96, 33.74, 30.67; HR-ESI-MS (DCM/MeOH): m/z calcd for $[\text{Fe}_4(\text{L}^9)](\text{PF}_6)_8$ $[\text{M} - 5\text{PF}_6]^{5+}$ 1262.4722, found 1262.4823; calcd for $\{[\text{Fe}_4(\text{L}^9)](\text{PF}_6)_7\}^{6+}, [\text{M} - 6\text{PF}_6]^{6+}$ 1027.8994, found 1027.9021; calcd for $\{[\text{Fe}_4(\text{L}^9)](\text{PF}_6)_6\}^{7+}, [\text{M} - 7\text{PF}_6]^{7+}$ 860.3474, found 860.3631; calcd for $[\text{Fe}_4(\text{L}^9)]^{8+} [\text{M} - 8\text{PF}_6]^{8+}$ 734.6834, found 734.6956.

■ ASSOCIATED CONTENT

■ Supporting Information

Ligand synthesis, ¹H and ¹³C NMR, HR-ESI-MS data for all new materials, and details of the structure determination of $[\text{Fe}_2(\text{L}^7)] \cdot 4\text{PF}_6 \cdot 30\text{DMSO}$. The Supporting Information is available free of charge on the ACS Publications website at DOI: 10.1021/acs.inorgchem.5b00940. CCDC-1020976 contains the supplementary crystallographic data for $[\text{Fe}_2(\text{L}^7)] \cdot 4\text{PF}_6 \cdot 30\text{DMSO}$, which can be obtained free of charge from The Cambridge Crystallographic Data Centre via www.ccdc.cam.ac.uk/data_request/cif.

■ AUTHOR INFORMATION

Corresponding Authors

*E-mail: christopher.glasson@jcu.edu.au.

*E-mail: Len.lindoy@sydney.edu.au.

Notes

The authors declare no competing financial interest.

■ ACKNOWLEDGMENTS

The authors thank the Australian Research Council for support.

■ REFERENCES

- (1) (a) Chakrabarty, R.; Mukherjee, P. S.; Stang, P. J. *Chem. Rev.* **2011**, *111*, 6810–6918. (b) Smulders, M. M. J.; Riddell, I. A.; Browne, C.; Nitschke, J. R. *Chem. Soc. Rev.* **2013**, *42*, 1728–1754.
- (2) (a) Leigh, D. A.; Pritchard, R. G.; Stephens, A. J. *Nat. Chem.* **2014**, *6*, 978–982. (b) Lindoy, L. F.; Park, K.-M.; Lee, S. S. *Chem. Soc. Rev.* **2013**, *42*, 1713–1727. (c) Sato, Y.; Yamasaki, R.; Saito, S. *Angew. Chem., Int. Ed.* **2009**, *48*, 504–507. (d) Niu, Z. B.; Gibson, H. W. *Chem. Rev.* **2009**, *109*, 6024–6046. (e) Megiatto, J. D.; Schuster, D. I. *Chem.—Eur. J.* **2009**, *15*, 5444–5448. (f) Leigh, D. A.; Lusby, P. J.; McBurney, R. T.; Morelli, A.; Slawin, A. M. Z.; Thomson, A. R.; Walker, D. B. *J. Am. Chem. Soc.* **2009**, *131*, 3762–3771. (g) Faiz, J. A.; Heitz, V.; Sauvage, J.-P. *Chem. Soc. Rev.* **2009**, *38*, 422–442.
- (3) (a) Schouwey, C.; Scopelliti, R.; Severin, K. *Chem.—Eur. J.* **2013**, *19*, 6274–6281. and references therein. (b) Mosquera, J.; Zorra, S.; Nitschke, J. R. *Angew. Chem., Int. Ed.* **2014**, *53*, 1556–1559. (c) Meng, W.; Ronson, T. K.; Clegg, J. K.; Nitschke, J. R. *Angew. Chem., Int. Ed.* **2013**, *52*, 1017–1021. (d) Caulder, D. L.; Powers, R. E.; Parac, T. N.; Raymond, K. N. *Angew. Chem., Int. Ed.* **1998**, *37*, 1840–1843. (e) Mugridge, J. S.; Bergman, R. G.; Raymond, K. N. *Angew. Chem., Int. Ed.* **2010**, *49*, 3635–3637. (f) Pluth, M. D.; Bergman, R. G.; Raymond, K. N. *Science* **2007**, *316*, 85–88.
- (4) (a) Huang, S. L.; Lin, Y. J.; Hor, T. S. A.; Jin, G. X. *J. Am. Chem. Soc.* **2013**, *135*, 8125–8128. (b) Ayme, J. F.; Beves, J. E.; Campbell, C. J.; Leigh, D. A. *Chem. Soc. Rev.* **2013**, *42*, 1700–1721. (c) Forgan, R. S.; Sauvage, J. P.; Stoddart, J. F. *Chem. Rev.* **2011**, *111*, 5434–5464. (d) Meyer, C. D.; Forgan, R. S.; Chichak, K. S.; Peters, A. J.; Tangchaivang, N.; Cave, G. W. V.; Khan, S. I.; Cantrill, S. J.; Stoddart, J. F. *Chem.—Eur. J.* **2010**, *16*, 12570–12581.
- (5) (a) Ward, M. D.; Raithby, P. R. *Chem. Soc. Rev.* **2013**, *42*, 1619–1636. (b) Ferguson, A.; Squire, M. A.; Siretanu, D.; Mitcov, D.; Mathoniere, C.; Clerac, R.; Kruger, P. E. *Chem. Commun.* **2013**, *49*, 1597–1599. (c) Bilbeisi, R. A.; Zorra, S.; Feltham, H. L. C.; Jameson, G. N. L.; Clegg, J. K.; Brooker, S.; Nitschke, J. R. *Chem.—Eur. J.* **2013**, *19*, 8058–8062. (d) Ronson, T. K.; Giri, C.; Beyeh, N. K.; Minkinen, A.; Topic, F.; Holstein, J. J.; Rissanen, K.; Nitschke, J. R. *Chem.—Eur. J.* **2013**, *19*, 3374–3382. (e) Liu, T. F.; Liu, Y.; Xuan, W. M.; Cui, Y. *Angew. Chem., Int. Ed.* **2010**, *49*, 4121–4124. (f) Saha, S.; Stoddart, J. F. *Chem. Soc. Rev.* **2007**, *36*, 77–92. (g) Champin, B.; Mobian, P.; Sauvage, J.-P. *Chem. Soc. Rev.* **2007**, *36*, 358–366. (h) Lützen, A. *Angew. Chem., Int. Ed.* **2005**, *44*, 1000–1002.
- (6) Perkins, D. F.; Lindoy, L. F.; McAuley, A.; Meehan, G. V.; Turner, P. *Proc. Nat. Acad. Sci. U.S.A.* **2006**, *103*, 532–537.

- (7) Glasson, C. R. K.; Meehan, G. V.; Motti, C. A.; Clegg, J. K.; Turner, P.; Jensen, P.; Lindoy, L. F. *Dalton Trans.* **2011**, *40*, 10481–10490.
- (8) Glasson, C. R. K.; Meehan, G. V.; Motti, C. A.; Clegg, J. K.; Turner, P.; Jensen, P.; Lindoy, L. F. *Dalton Trans.* **2011**, *40*, 12153–12159.
- (9) Glasson, C. R. K.; Meehan, G. V.; Clegg, J. K.; Lindoy, L. F.; Smith, J. A.; Keene, F. R.; Motti, C. *Chem.—Eur. J.* **2008**, *14*, 10535–10538.
- (10) Glasson, C. R. K.; Clegg, J. K.; McMurtrie, J. C.; Meehan, G. V.; Lindoy, L. F.; Motti, C. A.; Moubaraki, B.; Murray, K. S.; Cashion, J. D. *Chem. Sci.* **2011**, *2*, 540–543.
- (11) Glasson, C. R. K.; Meehan, G. V.; Clegg, J. K.; Lindoy, L. F.; Turner, P.; Duriska, M. B.; Willis, R. *Chem. Commun.* **2008**, 1190–1192.
- (12) Perkins, D. F.; Lindoy, L. F.; Meehan, G. V.; Turner, P. *Chem. Commun.* **2004**, 152–153.
- (13) SPARTAN '14; Wavefunction, Inc: Irvine, CA, 2014.